Supporting Information

MoS_2 Quantum Dots as Efficient Electrocatalyst for Hydrogen Evolution Reaction Over Wide pH Range.

Bishnupad Mohanty[1,2], Arijit Mitra[3], Bijayalaxmi Jena[2], Bikash Kumar Jena[1,4]*

[1]CSIR-Institute of Minerals and Materials Technology, Bhubaneswar-751013, India.

[2]Department of Chemistry, Utkal University, Bhubaneswar-751004, Odisha, India.

[3]Institute of Physics, Bhubaneswar-751005, India.

[4] Academy of Scientific & Innovative Research (AcSIR), Ghaziabad-201002, India

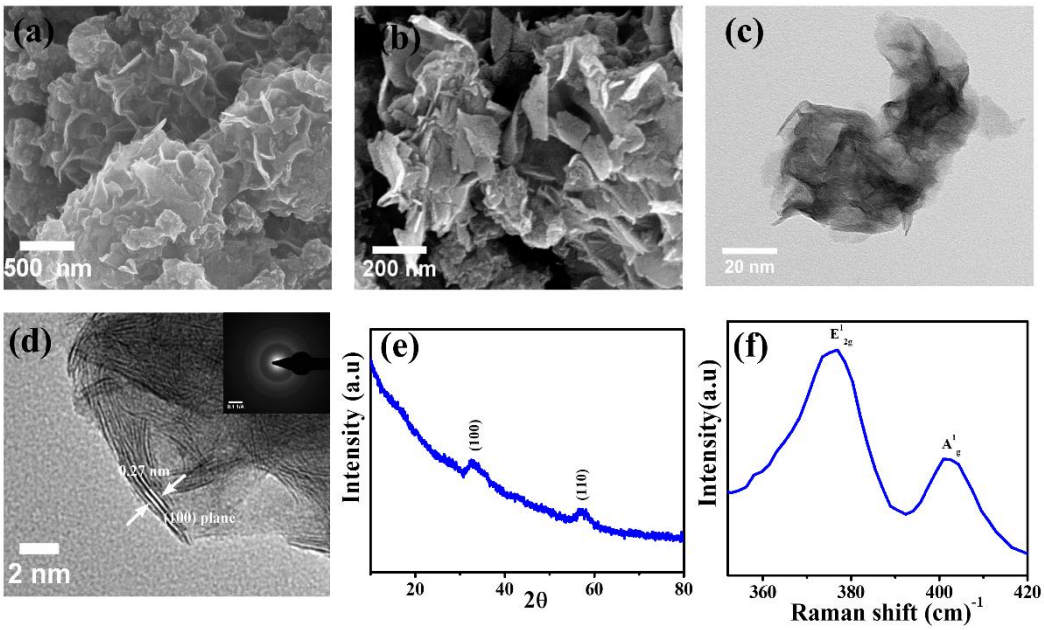

Figure S1. Characterization of MSNSs (a, b) FESEM image of MSNSs (c, d) TEM and HRTEM image of MSNSs (e) XRD pattern of MSNSs (f) Raman spectra MSNSs.

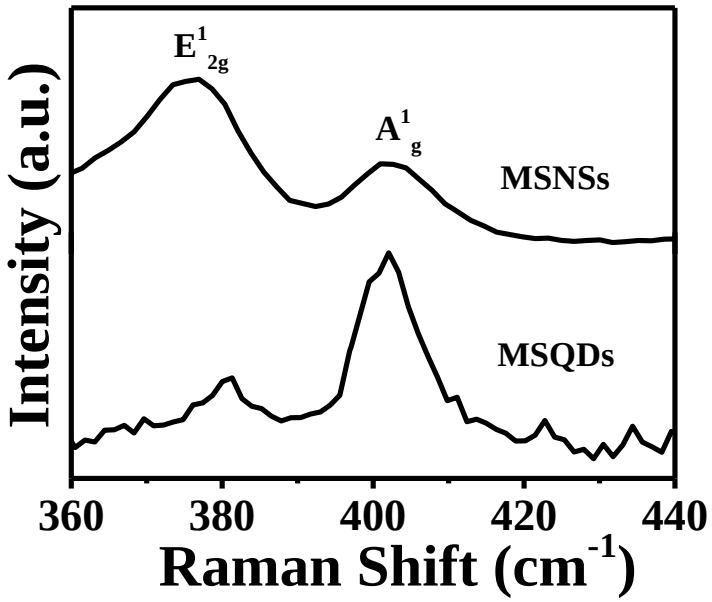

Figure S2. Raman spectra comparison of MSQDs and MSNSs.

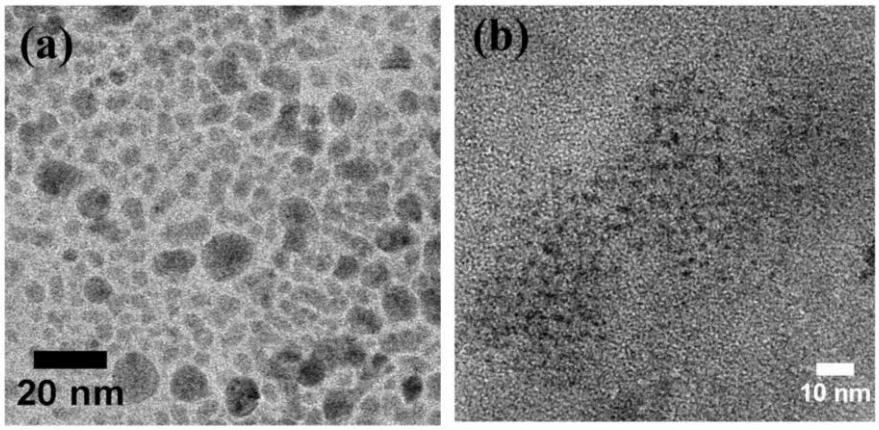

Figure S3. (a) TEM image of (a) MSQDs@CQDs and (b)CQDs

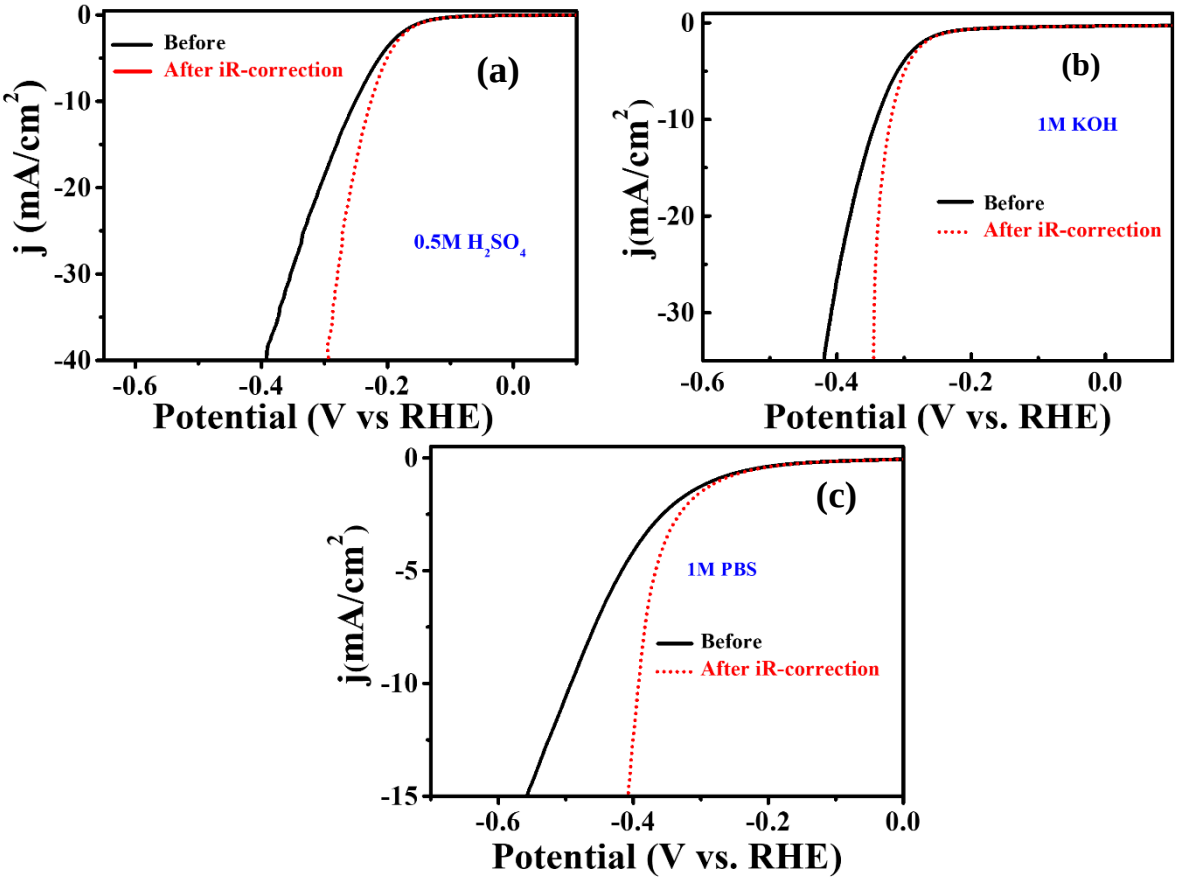

Figure S4. LSV data of MSQDs in before and after iR-correction of all the electrocatalysts (a) H_2SO_4 (0.5M), (b) KOH (1M), and (c) PBS (1M).

The potential of the Ag/AgCl electrode is corrected with the RHE scale. For that experiment, the reference electrode Ag/AgCl has calibrated in H_2-saturated KOH (1M) solution by using Pt as the working electrode, Ag/AgCl as a reference electrode, and Pt wire as the counter electrode. Before the measurement, the Pt electrode is pre-treated with H_2SO_4 (0.5M). The LSV has been recorded at a scan rate of 1 mV/sec. The potential at which the current crosses the zero line is taken as the correction factor. As shown in Figure S5, the current crosses the zero line at the potentials of -1.035 V. So, the correction factor for the Ag/AgCl reference electrode is 1.035 V.

So, E(RHE) = E (Ag/AgCl) + 1.035V

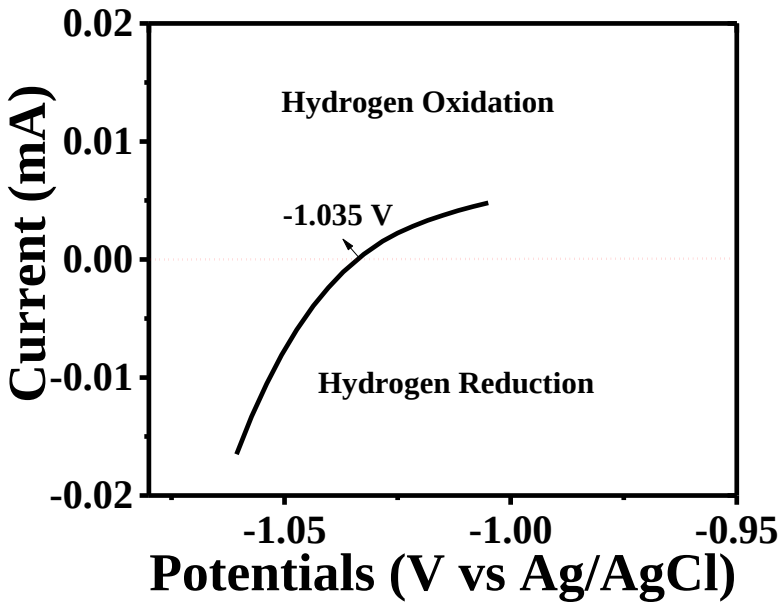

Figure S5. LSV showing the calibration of the Ag/AgCl reference electrode in KOH (1M) solution.

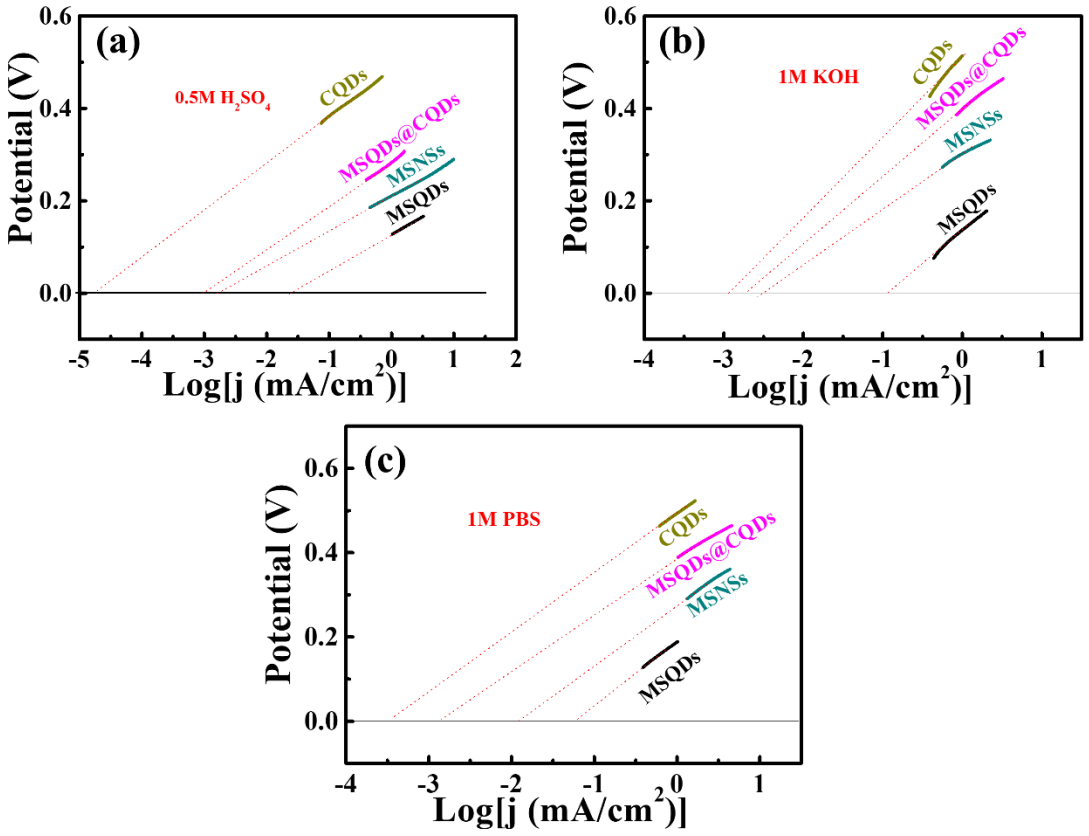

Figure S6. Exchange current density of all the electrocatalysts (a) H_2SO_4 (0.5M), (b) KOH (1M), and (c) PBS (1M).

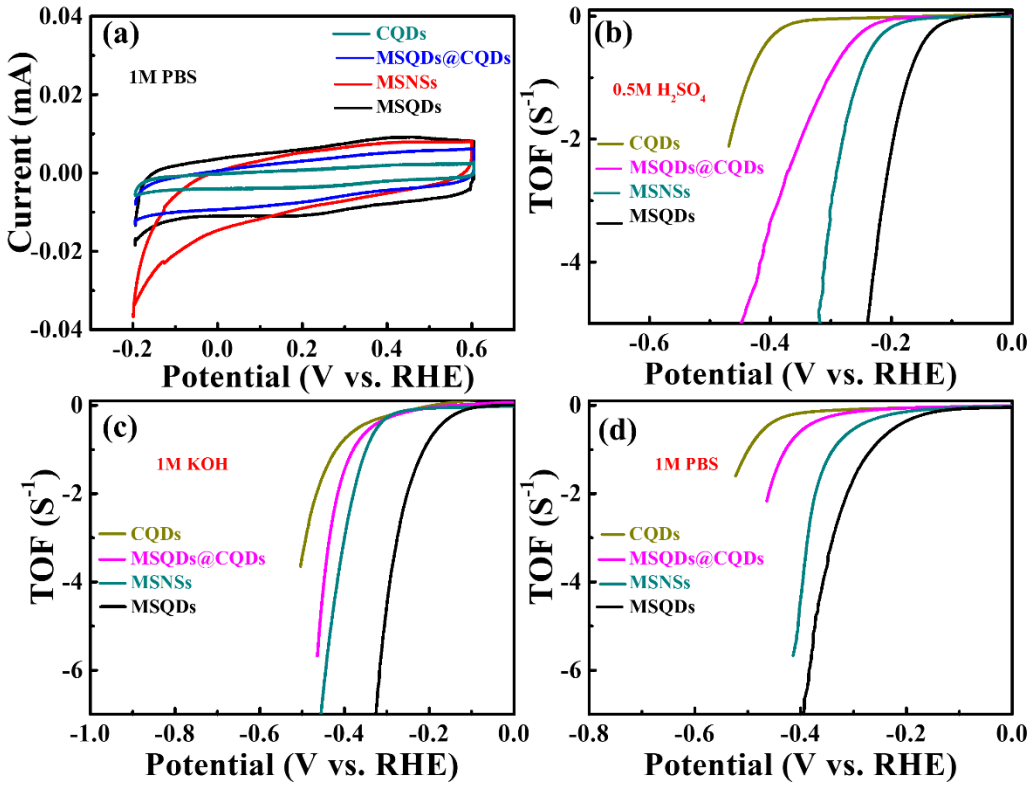

Figure S7. (A) CVs of as-synthesised materials in phosphate buffer (pH = 7) at a scan rate of 50 mV/s. (B, C, D) are TOF plot of different as-synthesized catalysts towards HER in H_2SO_4 (0.5M), KOH (1M), and PBS (1M) respectively.

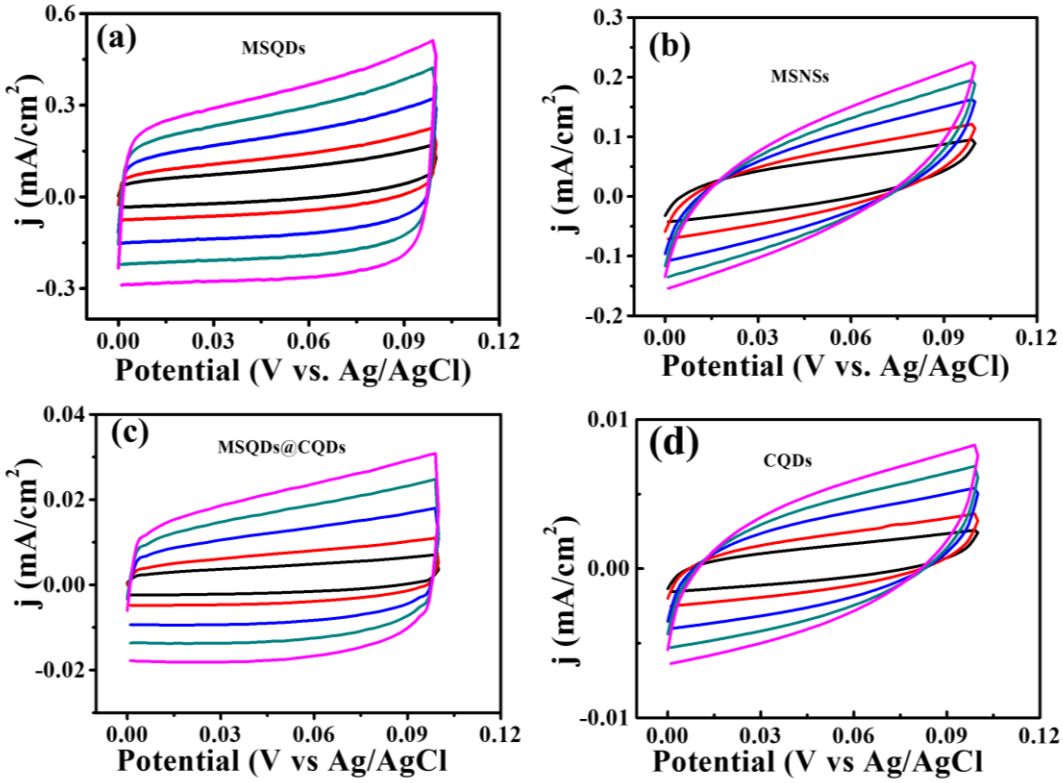

Figure S8. Cyclic voltammograms obtained from the non-Faradic Region of as-synthesized materials at different scan rates in H_2SO_4 (0.5M).

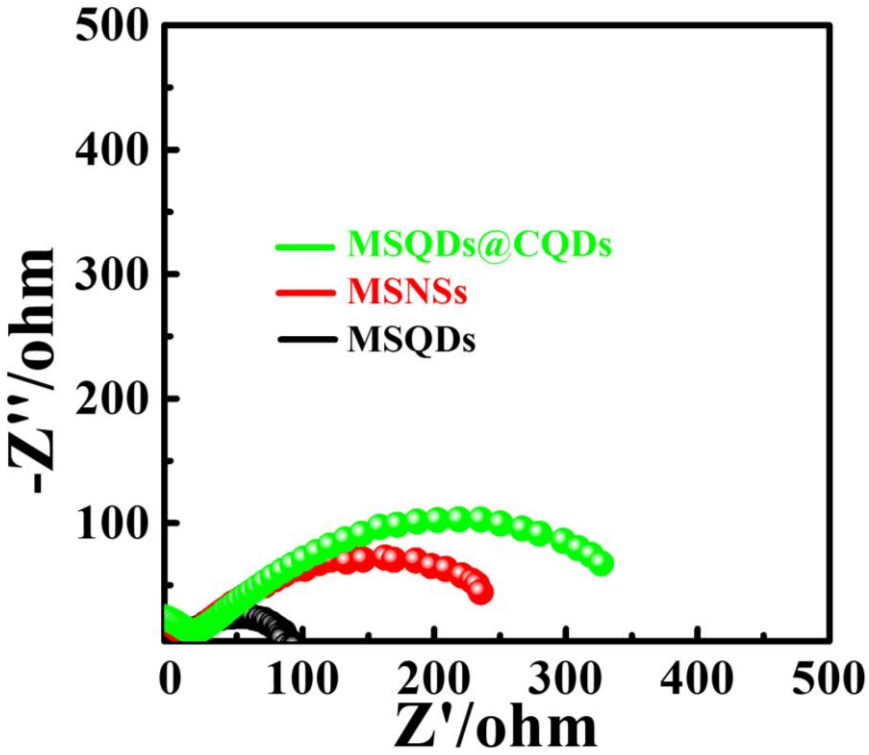

Figure S9. Nyquist plot of MSQDs, MSNSs and MSQDs@CQDs in H_2SO_4 (0.5M).

Table S1. Comparison table of η_{10}, Tafel slope, TOF, ECSA and R_f of all the catalysts in H_2SO_4 (0.5M)

Catalysts	η_{10} (mV)	Tafel slope (mV/dec)	TOF (s^{-1}) at η_{150}	ECSA (cm^2)	R_f
MSQDs	210	65	0.5	90	1267.6
MSNSs	305	81	0.054	20	281.7
MSQDs@CQDs	440	110	0.020	5.75	80.9
CQDs	-	180	0.007	1.22	17.2

Table S2. Performance comparison MSQDs towards HER in 0.5M H_2SO_4

Serial No.	Materials	Onset Potential (mV)	η_{10} (mV)	Tafel slope (mV/dec)	Ref.
1	rGO/MoS_2-S	160	250	72	**S**[1]
2	MoS_2 nanoflower/rGO	190	-	95	**S**[2]
3	MoS_2/NGP aerogels	236	261	230	**S**[3]
4	MoS_2 QDs on MoS_2 sheet	190	-	74	**S**[4]
5	Luminescent MoS_2 QDs	210	-	60	**S**[5]
6	Monolayer MoS_2 QDs	160	-	58	**S**[6]
7	MoS_2 nonodots/rGO	-	222	59.8	**S**[7]
8	AS-rich MoS_2 nanosheet	180	220	68	**S**[8]
9	MoP-graphite	100	300	63	**S**[9]

10	MoO_3-MoS_2 nanowires	200	254	60	**S**[10]
11	Double-gyroid MoS_2	150-200	206	50	**S**[11]
12	Ammoniated MoS_2	-	325	45	**S**[12]
12	MSQDs	130	210	65	This Work

Table S3. Comparison table of η_{10}, Tafel slope, TOF, ECSA and R_f of all the catalysts in KOH (1M)

Catalysts	**η_{10} (mV)**	**Tafel slope (mV/dec)**	**TOF (s^{-1}) at η_{150}**
MSQDs	270	80	0.20
MSNSs	405	94	0.050
MSQDs@CQDs	455	110	0.008
CQDs	-	180	0.001

Table S4. Performance comparison MSQDs towards HER in KOH (1M)

Serial No.	**Materials**	**Onset Potential (mV)**	**η_{10} (mV)**	**Tafel slope (mV/dec)**	**Ref.**
1	Ni_2P	-	250	100	**S**[13]
2	$NiCo_2S_4$ NW/NF	-	310	58.9	**S**[14]
3	Co-P/Co-PO_4	220	380	-	**S**[15]
4	Co_7Se_8	317	472	59.1	**S**[16]
5	EG/$Co_{0.85}$Se/NiFe-LDH	240	265	160	**S**[17]
6	$Ni(OH)_2$/Ti	-	290	190	**S**[18]
7	CoOx@CN	85	232	82	**S**[19]
8	Co NPs@NCNTs	160	370	82	**S**[20]
9	Mo_2C-Ni@NCNF	-	383	162	**S**[21]

10	Ni3S2 /MWCNT-NC	350	480	102	**S**[22]
11	MSQDs	155	270	78	This Work

Table T5. Comparison table of η_{10}, Tafel slope, TOF, ECSA and R_f of all the catalysts in PBS (1M)

Catalysts	**η_{10} (mV)**	**Tafel slope (mV/dec)**	**Exchange current density (j_0)**	**TOF (s^{-1}) at η_{150}**
MSQDs	335	116	0.056	0.172
MSNSs	390	138	0.112	0.059
MSQDs@CQDs	-	145	0.0012	0.32
CQDs	-	162	0.0033	0.0045

Table S6. Performance comparison MSQDs towards HER in PBS (1M)

Serial No.	**Materials**	**Onset Potential (mV)**	**η_{10} (mV)**	**Tafel slope (mV/dec)**	**Ref.**
1	MoS_3 on glassy carbon	171-203	-	86	**S**[23]
2	WP_2 nanorods	172	298	79	**S**[24]
3	MoS_2/NGP aerogel	236	261	230	**S**[3]
4	$CuMoS_4$	135	337	95	**S**[25]
5	$CoO/CoSe_2$	200	337	131	**S**[26]
6	$CoMoS_4$	152	420	253.7	**S**[27]
7	Co-NRCNTs	330	540	-	**S**[20]
8	CoS_2/CNF	130	360	163.7	**S**[28]

9	Ni-S	237	337	77	**S**[29]
10	$Mn_3(PO_4)_2 \cdot 3H_2O$/FTO	450	680	120	**S**[30]
11	FeP@NPC	-	386	67	**S**[31]
12	MSQDs	200	335	116	This Work

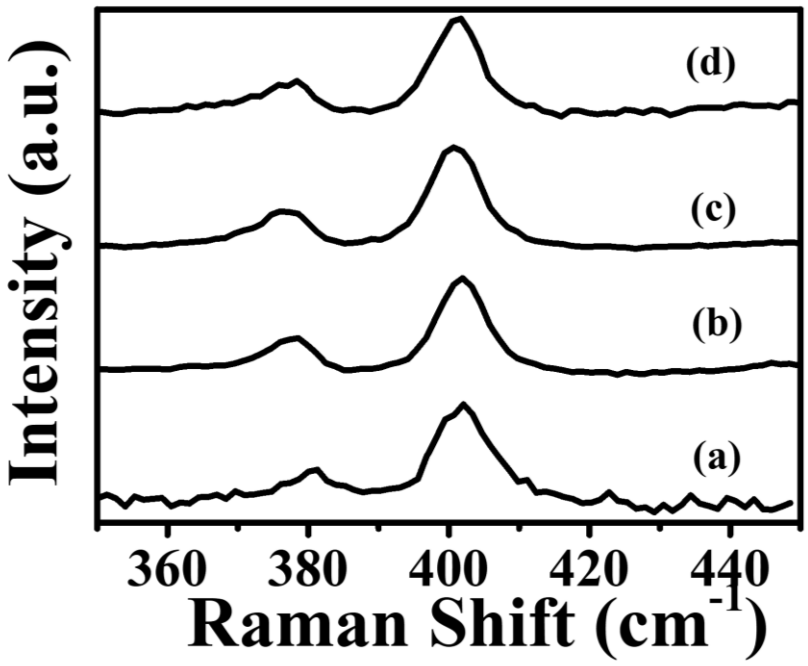

Figure S10. Raman spectra of MSQDs before (a) and after stability measurement in H_2SO_4 (0.5M) (b), KOH (1M) (c) and PBS (1M) solution (d).

Reference

(1) Kamila, S.; Mohanty, B.; Samantara, A. K.; Guha, P.; Ghosh, A.; Jena, B.; Satyam, P. V; Mishra, B. K.; Jena, B. K. Highly Active 2D Layered MoS2-rGO Hybrids for Energy Conversion and Storage Applications *Sci. Rep.* **2017**, *7*, 8378.

(2) Ma, C.-B.; Qi, X.; Chen, B.; Bao, S.; Yin, Z.; Wu, X.-J.; Luo, Z.; Wei, J.; Zhang, H.-L.; Zhang, H. MoS_2 nanoflower-decorated reduced graphene oxide paper for high-performance hydrogen evolution reaction *Nanoscale* **2014**, *6*, 5624–5629.

(3) Hou, Y.; Zhang, B.; Wen, Z.; Cui, S.; Guo, X.; He, Z.; Chen, J. A 3D hybrid of layered MoS2/nitrogen-doped graphene nanosheet aerogels: an effective catalyst for hydrogen evolution in microbial electrolysis cells *J. Mater. Chem. A* **2014**, *2* , 13795–13800.

(4) Gopalakrishnan, D.; Damien, D.; Shaijumon, M. M. MoS_2 Quantum Dot-Interspersed Exfoliated MoS_2 Nanosheets. *ACS Nano* **2014**, *8*, 5297–5303.

(5) Gopalakrishnan, D.; Damien, D.; Li, B.; Gullappalli, H.; Pillai, V. K.; Ajayan, P. M.; Shaijumon, M. M. Electrochemical synthesis of luminescent MoS_2 quantum dots *Chem. Commun.* **2015**, *51*, 6293–6296.

(6) Ren, X.; Pang, L.; Zhang, Y.; Ren, X.; Fan, H.; Liu, S. (Frank). One-step hydrothermal synthesis of monolayer MoS2 quantum dots for highly efficient electrocatalytic hydrogen evolution. *J. Mater. Chem. A* **2015**, *3*, 10693–10697.

(7) Sun, W.; Li, P.; Liu, X.; Shi, J.; Sun, H.; Tao, Z.; Li, F.; Chen, J. Size-controlled MoS2 nanodots supported on reduced graphene oxide for hydrogen evolution reaction and sodium-ion batteries. *Nano Research* **2017**, *10*, 2210–2222.

(8) Benson, J.; Li, M.; Wang, S.; Wang, P.; Papakonstantinou, P. Electrocatalytic Hydrogen Evolution Reaction on Edges of a Few Layer Molybdenum Disulfide Nanodots. *ACS Appl. Mater.Inter.* **2015**, *7*, 14113–14122.

(9) Jyothirmayee Aravind, S. S.; Ramanujachary, K.; Mugweru, A.; Vaden, T. D. Molybdenum phosphide-graphite nanomaterials for efficient electrocatalytic hydrogen production *Applied Catalysis A: General* **2015**, *490*, 101–107.

(10) Chen, Z.; Cummins, D.; Reinecke, B. N.; Clark, E.; Sunkara, M. K.; Jaramillo, T. F. Core–shell MoO_3–MoS_2 Nanowires for Hydrogen Evolution: A Functional Design for Electrocatalytic Materials. *Nano Letters* **2011**, *11*, 4168–4175.

(11) Kibsgaard, J.; Chen, Z.; Reinecke, B. N.; Jaramillo, T. F. Engineering the surface structure of MoS2 to preferentially expose active edge sites for electrocatalysis. *Nat Mater* **2012**, *11*, 963–969.

(12) Wu, Z.; Tang, C.; Zhou, P.; Liu, Z.; Xu, Y.; Wang, D.; Fang, B. Enhanced hydrogen evolution catalysis from osmotically swollen ammoniated MoS_2. *J. Mater. Chem. A* **2015**, *3*, 13050–13056.

(13) Feng, L.; Vrubel, H.; Bensimon, M.; Hu, X. Easily-prepared dinickel phosphide (Ni2P) nanoparticles as an efficient and robust electrocatalyst for hydrogen evolution. *Phy Chem Chem Phy.* **2014**, *16*, 5917–5921.

(14) Sivanantham, A.; Ganesan, P.; Shanmugam, S. Hierarchical NiCo2S4 Nanowire Arrays Supported on Ni Foam: An Efficient and Durable Bifunctional Electrocatalyst for Oxygen and Hydrogen Evolution Reactions. *Adv. Funct. Mater.* **2016**, *26*, 4661–4672.

(15) Yang, Y.; Fei, H.; Ruan, G.; Tour, J. M. Porous Cobalt-Based Thin Film as a Bifunctional Catalyst for Hydrogen Generation and Oxygen Generation. *Adv. Mater.* **2015**, *27*, 3175–3180.

(16) Masud, J.; Swesi, A. T.; Liyanage, W. P. R.; Nath, M. Cobalt Selenide Nanostructures: An Efficient Bifunctional Catalyst with High Current Density at Low Coverage. *ACS Appl. Mater.Inter.* **2016**, *8* , 17292–17302.

(17) Hou, Y.; Lohe, M. R.; Zhang, J.; Liu, S.; Zhuang, X.; Feng, X. Vertically oriented cobalt selenide/NiFe layered-double-hydroxide nanosheets supported on exfoliated graphene foil: an efficient 3D electrode for overall water splitting. *Energy Envirn. Sci.* **2016**, *9*, 478–483.

(18) Danilovic, N.; Subbaraman, R.; Strmcnik, D.; Chang, K.-C.; Paulikas, A. P.; Stamenkovic, V. R.; Markovic, N. M. Enhancing the Alkaline Hydrogen Evolution Reaction Activity through the Bifunctionality of Ni(OH)2/Metal Catalysts. *Angew. Chem. Int. Ed.* **2012**, *51*, 12495–12498.

(19) Jin, H.; Wang, J.; Su, D.; Wei, Z.; Pang, Z.; Wang, Y. In situ Cobalt–Cobalt Oxide/N-Doped Carbon Hybrids As Superior Bifunctional Electrocatalysts for Hydrogen and Oxygen Evolution. *J. Am. Chem. Soc.* **2015**, *137*, 2688–2694.

(20) Zou, X.; Huang, X.; Goswami, A.; Silva, R.; Sathe, B. R.; Mikmeková, E.; Asefa, T. Cobalt-Embedded Nitrogen-Rich Carbon Nanotubes Efficiently Catalyze Hydrogen Evolution Reaction at All pH Values. *Angew. Chem. Int. Ed.* **2014**, *53*, 4372–4376.

(21) Tang, Y.; Li, W.; Jiao, L.; Li, F.; Yang, Y.; Wang, X.; Gao, W.; Li, R. Mo2C-Ni-modified nitrogen-doped carbon nanofiber toward efficient hydrogen evolution reaction *New Journal of Chemistry* **2017**, *41*, 12956–12961.

(22) Lin, T.-W.; Liu, C.-J.; Dai, C.-S. Ni3S2/carbon nanotube nanocomposite as electrode material for hydrogen evolution reaction in alkaline electrolyte and enzyme-free glucose detection. *Appl. Catal. B: Environ.* **2014**, *154*, 213–220.

(23) Merki, D.; Vrubel, H.; Rovelli, L.; Fierro, S.; Hu, X. Fe, Co, and Ni ions promote the catalytic activity of amorphous molybdenum sulfide films for hydrogen evolution. *Chem. Sci.* **2012**, *3*, 2515–2525.

(24) Du, H.; Gu, S.; Liu, R.; Li, C. M. Tungsten diphosphide nanorods as an efficient catalyst for electrochemical hydrogen evolution. *Journal of Power Sources* **2015**, *278*, 540–545.

(25) Tran, P. D.; Nguyen, M.; Pramana, S. S.; Bhattacharjee, A.; Chiam, S. Y.; Fize, J.; Field, M. J.; Artero, V.; Wong, L. H.; Loo, J.; Barber,J. Copper molybdenum sulfide: a new efficient electrocatalyst for hydrogen production from water . *Energy Environ. Sci.* **2012**, *5*, 8912–8916.

(26) Li, K.; Zhang, J.; Wu, R.; Yu, Y.; Zhang, B. Anchoring CoO Domains on CoSe2 Nanobelts as Bifunctional Electrocatalysts for Overall Water Splitting in Neutral Media. *Adv. Sci.* **2016**, *3*, 1500426.

(27) Shao, L.; Qian, X.; Wang, X.; Li, H.; Yan, R.; Hou, L. Low-cost and highly efficient CoMoS4/NiMoS4-based electrocatalysts for hydrogen evolution reactions over a wide pH range. *Electrochimica Acta* **2016**, *213*, 236–243.

(28) Gu, H.; Huang, Y.; Zuo, L.; Fan, W.; Liu, T. Electrospun carbon nanofiber@CoS2 core/sheath hybrid as an efficient all-pH hydrogen evolution electrocatalyst. *Inorganic*

Chemistry Frontiers **2016**, *3*, 1280–1288.

(29) Jiang, N.; Bogoev, L.; Popova, M.; Gul, S.; Yano, J.; Sun, Y. Electrodeposited nickel-sulfide films as competent hydrogen evolution catalysts in neutral water. *J. Mater. Chem. A* **2014**, *2* , 19407–19414.

(30) Jin, K.; Park, J.; Lee, J.; Yang, K. D.; Pradhan, G. K.; Sim, U.; Jeong, D.; Jang, H. L.; Park, S.; Kim, D.; Sung, N.-E.; Kim, S. H.; Han, S.; Nam, K. T. Hydrated Manganese(II) Phosphate (Mn3(PO4)2·3H2O) as a Water Oxidation Catalyst. *J. Am. Chem. Soc.* **2014**, *136*, 7435–7443.

(31) Pu, Z.; Amiinu, I. S.; Zhang, C.; Wang, M.; Kou, Z.; Mu, S. Phytic acid-derivative transition metal phosphides encapsulated in N,P-codoped carbon: an efficient and durable hydrogen evolution electrocatalyst in a wide pH range. *Nanoscale* **2017**, *9*, 3555–3560.